Available online at www.sciencedirect.com

ScienceDirect

Procedia Engineering 99 (2015) 1514 – 1525

Procedia Engineering

www.elsevier.com/locate/procedia

"APISAT2014", 2014 Asia-Pacific International Symposium on Aerospace Technology, APISAT2014

A Numerical investigation of the Sparkjet Actuator in Multiple – shot Mode

Lv Yuanwei,Shan Yong, Zhang Jingzhou,Tan Xiaoming *

Jiangsu Province Key Laboratory of Aerospace Power Systems, College of Energy and Power, Nanjing University of Aeronautics and Astronautics, Nanjing 210016, China

Abstract

Computational simulations were performed in multiple-shot mode to investigate the effects of the boundary conditions and the deposition energy on the performance of the Sparkjet actuator. The user define function (UDF) was applied in the source term of the energy equation to imitate the very arc current discharges which produce the synthetic flow. The method of numerical simulation is verified by the existing experimental and analytical data. Two parameters including the integration mass and momentum are defined to evaluate the performance of the Sparkjet actuator. The simulation results show that Sparkjet flow is more affected by the boundary conditions of the external walls of the cavity and its deposition energy. The performance of Sparkjet actuator drops with the increase of operation cycle when the wall of cavity is adiabatic. When the temperature of wall of cavity is constant, the integration mass and momentum during the exhaling stage decrease with the increase of temperature. The performance of actuator decreases with the increase of heat transfer coefficient when the wall of cavity is set to be coupled with effect of radiation and convection. The performance of actuator increases with increase of deposition energy.

Peer-review under responsibility of Chinese Society of Aeronautics and Astronautics (CSAA)

Keywords: Sparkjet actuator; multiple-shot; numerical simulation; boundary conditions and deposition energy

1. Introduction

Flow control technology is the hotspot and front of research on modern fluid dynamics. Effective flow control system and devices have played a significance role in the security of aircraft, maneuverability improving and the

* Corresponding author. Tel.: +86-15651875785; .
E-mail address: lvyuanwei@nuaa.edu.com

Peer-review under responsibility of Chinese Society of Aeronautics and Astronautics (CSAA)
doi:10.1016/j.proeng.2014.12.703

efficiency of propulsion enhancement. The operation of executive implement, as the core of flow control, is constrained by design, operation parameters and environment and it determines the application areas and potency. Traditional passive flow control method has not meet broader operation scope and harsh running environment. The active flow control methods, the synthetic jet, have attracted a large number of researchers from various fields include delaying separation of boundary layer, aircraft lift elevation and mixture enhancement during the last decade.

A synthetic jet [1] is a semi-steady jet of fluid generated from the pressure (or density or temperature) difference in flow field between the cavity and environment because of the energy loading in the cavity with orifice, its execution equipment is the synthetic jet actuator. A synthetic jet is superior over a continuous jet because of the characteristic of low cost and size, the ability of penetrating supersonic boundary layers and zero-net-mass-flux and controlling easily. Various kinds of actuators have been proposed and developed in recently ten years for different use in low-speed flows [2-7]. Their stimulation source includes a moving piston-driven [8], piezoelectric-driven [9] and plasma-driven [10]. Though these actuators have been more successfully employed in the low-speed flow for different regimes, it scarcely solves the separation of the boundary layers in the subsonic, transonic, supersonic and hypersonic flow.

A new actuator for high-speed flow control, the Sparkjet actuator, is developed by The Johns Hopkins University Applied Physics Laboratory (JHU/APL) in 2004[11]. Its mechanism is that a supersonic flow is generated from discharge of one or several electrodes located in the cavity with orifice(s). The schematic of the Sparkjet actuator is seen as the Figure. 1. In the cavity of the Spark Jet actuator, one or several electrode with high voltage discharge and heat the air inner the cavity, then the temperature and pressure of the air increases in microseconds and expulses outward the environment through the orifice.

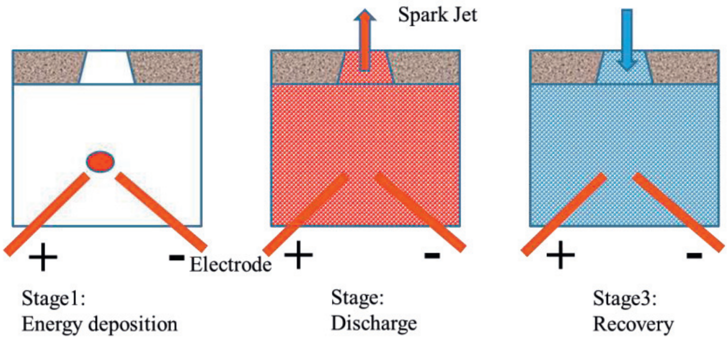

Fig.. 1. Sparkjet Operating Schematic [11].

There are some computational and experimental studies of the Sparkjet actuator for flow control and parameters optimizing. K. R. Grossman et al [11] conducted that the performance and sensitivities of single-pulse the sparkjet actuator is affected by the orifice diameter, chamber volume, and energy deposited, that is, less orifice diameter and chamber volume and larger deposition energy is good to the conforming of sparkjet. B. Z. Cybyk et al[12] experimented that sparkjet can penetrate a fully developed supersonic boundary layer with a Mach 3 cross flow, which is measured by Laser Doppler Velocimetry (LDV) and Particle Imaging Velocimetry (PIV) and attests the potential of flow control when operating in a single-pulse mode. Wang Lin et al [13] based on the Joule heating effect of gas discharge, obtained the fractions of power and jet kinetic energy with numerical methods and come up with saturation frequency which represents the ability of outsider air backfill the cavity. Yong SHAN et al [14] employ user define function (UDF) as the source term to simulate the discharge of electrode in order to gain the characteristic of multiple stimulation numerically and found increasing of operation frequency will lower the time which is used for cooling the cavity and it exists a optimizing frequency for the actuator, the higher heat resistance and better heat transfer measure should be considered. Yuanwei LV et al [15] investigated the effects of the boundary conditions (temperature, convection, radiation and adiabatic walls) of the external walls of the cavity and the operation parameters (energy deposition values and the time of deposition) in signal-pulse mode to substantiate that the boundary conditions of walls of cavity and operation parameters have a significant impact on the performance of actuator. B. Z. Cybyk et al [16] focuses on the detailed characteristics of the Sparkjet's discharge and cooling stages after a single energy deposition pulse which consists of three distinct stages: energy deposition, discharge, and recovery. Sarah J Haack et al [17] obtained an analytical solution to evaluate the performance of actuator and demonstrate that a maximum efficiency factor of 35% for Sparkjet actuators. S. J. Haack [18] revealed an operating efficiency of 20-30% at atmospheric pressures through three experimental techniques: cavity pressure measurements, high-quality micro-Schlieren images acquisition for velocity and Joule heat measurements.

Previous researchers obtained initial characteristics of Sparkjet actuators and tested and verified the ability of flow control by large number of experiments and numerical simulations. However, some important factors such as the boundary conditions of walls in the cavity and the operation parameters for actuator design and application have not researched comprehensively and systematically in multiple–shot mode. This study will concentrate on the effective of the boundary conditions (include temperature, convection, radiation and adiabatic walls) of the inner the walls in the cavity and the deposition energy to the performance of multiple –shot mode Sparkjet actuators. Some indicators should be defined to evaluate the capability of actuator. Furthermore, most of the numerical studies in the past have simulated only a single case, over a limited operation range, with variation of one or two parameters such as deposition energy or operation frequency. There is therefore a need to study the effect of individual parameters separately and compare them with a baseline case; such results can be used for maximization of synthetic jet flow. Our study can reveal the characteristic and mechanism of Sparkjet actuators in multiple –shot mode.

2. Numerical simulation procedure

2.1. Numerical domain and mesh

The dimension of baseline actuator in this study are based on the experiment and simulation of B. Z. Cybyk[16]. The geometry of the baseline actuator included orifice diameters of 0.33mm, chamber volumes of 4.056E-8m3, and the detail values is shown in Figure. 2(a). The simulation domain of Sparkjet is divided into two regions: the first includes the cavity and orifice, and the second comprises the ambient air into which the jet exits (see Figure. 3). In studies for the effect of the ambient air near field of the jet, it is found that a domain size of 50mm (along the axis) and 30mm (in the lateral direction) is sufficient. For this domain size, jet near field parameters are not affected by boundary condition applied at the end of the outer region. The stimulation region need to be defined separately from other zooms in the cavity so that a user-defined function (UDF) can be used to describe the electric discharge between the Sparkjet anodes with cathode (Figure. 2(b)). It is good to input the parameters of energy deposition such as the magnitude of energy and duration time in energy deposition stage.

The total size of the grid was approximately 47374 cells. These include cavity of 18524, orifice of 300 and the out reign of 28552. 8 boundary layer meshes are concentrated near the surface of the cavity to refine the overall grid in the chamber. The grid of the outer reign is ensured that the maximum concentration of grid points is along the orifice and near the orifice exit. A 0.00825mm resolution at the orifice exit is found adequate for an orifice with a diameter of 0.33mm. The grid independence studies was also done, the average velocity of the orifice outlet changes of 35% when the total amount of grid has varied from 38562 to 47374, deviation of 0.1% occurred when the total amount of grid has varied from 47374 to 52084. For this gird (47374), the parameter of actuator will not be affected by the amount of gird.

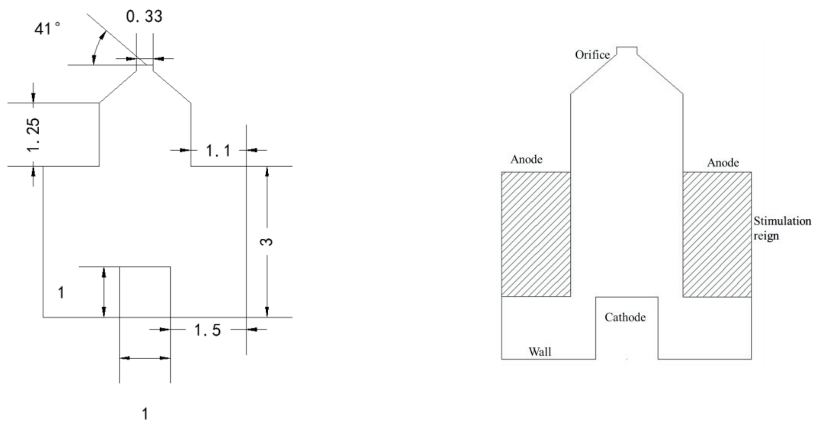

Fig. 2. Sparkjet actuator [9]:(a) the relevant geometric parameters and (b) the energy deposition region employed in the simulation domain.

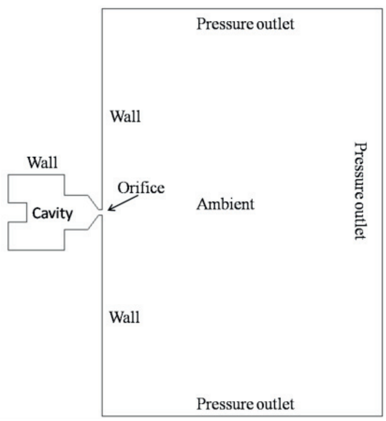

Fig. 3. the overall simulation domain and boundary conditions

2.2. Simulation set

The commercial package Fluent 6.3.2 is used for Sparkjet simulations and Gambit 2.1 for geometry and mesh generation. In the energy deposition reign, the electric discharge heats air and temperature (pressure) rise. The most challenging part in the simulation is imitation of the very arc current discharges. In this study, a user-defined function (UDF) as the source term is directly added in the energy conservation equation of Navier Stokes and supposes that this energy deposition is uniform and sustained in a short time(microseconds). In order to use source term reasonable, we do a series assumption as follow, all the energy which discharged between the cathode and anode is converted to the thermal and heat the air in the cavity in the energy deposition reign completely, that is the efficiency of the Sparkjet is 100%; the air in the cavity is ideal gas and the thermal conductivity and viscosity comply with the kinetic theory because of large range of temperature in the cavity; neglecting the ablation of electrode, which would increase the volume of the cavity, and the distribution of energy is uniform in the energy deposition reign.

Except parameters of deposition energy and geometry, the thermal environment around the actuator, that is boundary conditions of the surface inner the cavity, these include constant temperature, convection, radiation and adiabatic walls; influence heavily its performance especially for the kinds of high energy density Sparkjet actuators. The setup of boundary condition in the simulation domain is as follows: impenetrable wall of the surface of the cavity and orifice, pressure outlet of the outlet at the end of the outer region (the temperature is 300K and the pressure is 101325Pa), the outlet of orifice is designed to be interior face so that we can monitor the flow parameters through it. Referring to the experiment of B. Z. Cybyk[16], the deposition energy is 0.0302J and suppose the duration time in energy deposition stage is 1μs. The two are the baseline operating parameters in the study.

Reference to the previous experiment data, the Sparkjet flow is up to 400m/s and larger than sound speed [18] and larger pressure (velocity and temperature) gradients near the orifice, obviously, the flow field is in a intensive turbulent state. A k–ε RNG model, which is deduced by transient Navier Stokes equation, is been selected to predict the variation of temperature and Reynolds stress.

The computation is carried out by using the commercial CFD software FLUENT coupled with the user definition function (UDF) describing the process of discharge. The segregated, unsteady, swirl-symmetric solver is chosen with first-order implicit time scheme that is unconditionally stable with respect to time step size. The default of 100 maximum iterations per time step is kept. A time step of one tenth of the duration time in energy deposition stage is chosen. In the residual monitors, the convergence criteria are set as 10-5. Finishing one case costs about 48h. More details on these solvers could be found in the ANSYS Fluent Software User's Guide [19].

2.3. Numerical domain and mesh

There are three deviations in our numerical simulation model. Firstly, capacitive energy will also convert to kinetic energy of gas; molecular ionization energy and is not limited to localized thermal energy of gas, which means the efficiency of the Sparkjet is far less than 100% when the arc current discharge occurs in cavity [18]. Secondly, the arc discharge is formed by an unpredictable line and it fabrics a conformation of line heat sources while this stimulation model presuppose the uniform distribution of energy. The third deviation is different energy deposition in different operation cycle because of change of density, temperature and pressure accord to Paschen law. These factors which not match the actual condition will lead to the deviations of stimulation and experiment data. In fact, the computational values are larger than the measurement values. But Referring to the analytical of K.R.Grossman[17], the numerical simulation model is still agreeable to the trend of the experiment and Analytical Model, as shown in Figure. 4. The simulation means still can reveal the flow field mechanism when operating in a multiple-pulse mode.

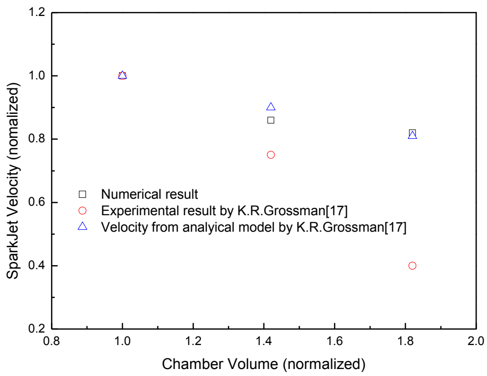

Fig. 4. validation of numerical simulation

2.4. Parameter definition

In order to evaluate the performance of Sparkjet actuators, some parameters are defined as follow:

(1) The first cycle time t_c[15]

The first cycle time t_c is the span of time that begins with the energy deposition and finishes with the velocity of the orifice drop to zero which air first flow in the cavity when operating in a single-pulse mode. The t_c include the time span of energy deposition stage, discharge stage and recovery stage which only when the backflow drop to zero firstly (see Figure. 5). At this time, the air mass influx the cavity is largest; it is the best time for the second-pulse. The t_c represent the ability of response and the degree of difficulty of "reset" of actuators. Smaller t_c means the faster response of the Sparkjet actuators.

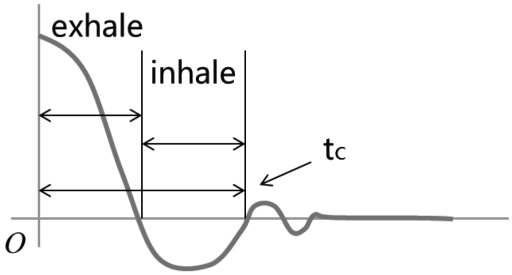

Fig. 5. the Schematic of the first cycle time

(2)The integration mass during the exhaling stage

The Sparkjet's carrier is gas from cavity, the magnitude of Sparkjet mass has a significant impact on the strength of jet when it is used for flow control and mixture enhancement. When actuators are operating in a multiple-pulse mode, the integration mass is defined the air mass exhaled through orifice within one working cycle. It is given by

$$m = \int_0^{t_{exhale}} \rho A \left| v_{average} \right| dt \tag{1}$$

t_{exhale} is the time span of energy deposition stage and discharge stage. The integration mass, the more violent of Sparkjet and the better performance of the actuator is.

To investigate the potency of the spark jet to "disturbance" to the outside flow field further or work to outside, we could define the integration momentum during the exhaling stage, it is expressed as:

$$P_{out} = \int_0^{t_{exhale}} m v_{average} dt \tag{2}$$

The integration momentum represents the capability of Sparkjet to penetrate the external flow field and do work. Larger integration momentum means the jet can transport to longer distances and carry more energy. The larger integration momentum, the stronger the spark jet working to the outside flow field further is and the better performance of the actuator is.

3. Results and analysis

Experimental determination of the effect of individual parameters is time consuming and expensive; nonetheless, it has been attempted by D. Caruana et al. [15]. Numerical simulations can provide results over a wide range of parameters with reasonable computational time and adequate flow resolution inside the cavity. For comparison between different shapes and sizes, a baseline case with parameters as given in Figure 2 is defined.

3.1. Effect of adiabatic walls

In this series of simulations, the energy deposition (0.0302J), duration of stimulation (1μs) and initial temperature (550K) of flow field were held constant. The wall of cavity is adiabatic for baseline actuator. The operation frequency varies from 100 mm to 1000 mm. the velocity of jet at the outlet of orifice versus time plot with operation frequency of 1000 Hz, the velocity of jet change cyclically with operation cycle and peak velocity per operation cycle increase. This is due to reducing of gas mass in the cavity increases the energy density in cavity. This is no heat transfer in walls and gas, the static temperature of jet continues to rise. it lead to the recovery stage do not take place because the velocity of jet is larger than zero throughout operation and no suck gas to supplement the gas loss during the exhaling stage if walls is adiabatic. Therefor the integration mass and peak Mach number would continue to drop (see Figure. 6(c) and (d)). The residues gas mass in the cavity has reduce to very small value when number of cycles is greater than 5. The integration momentum also continuously decreases (not shown). Figure. 6 concludes that an adiabatic wall of cavity is harmful to performance of actuator. In order to obtain the optimizational performance when put actuator to reality, good cooling condition should be considered and found.

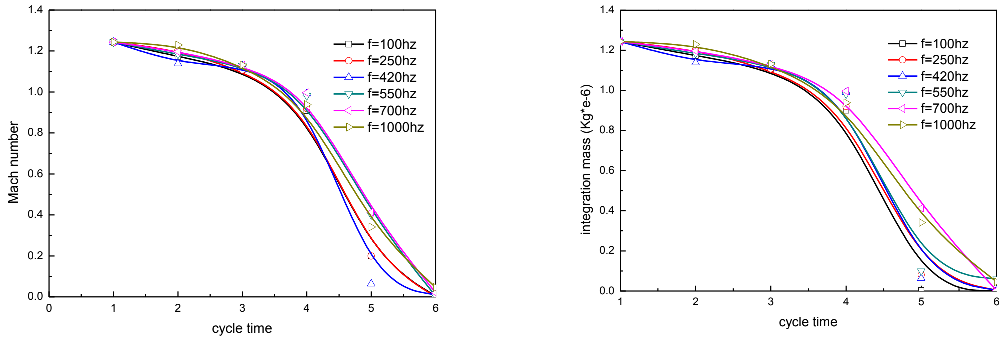

(a) peak Mach number versus time (b) the integration mass versus time

Fig. 6. effects of adiabatic walls

3.2. Effect of mixed boundary conditions (radiation + adiabatic walls)

Reality is heat transfer mechanism in walls of cavity and environment includes convection and radiation. Simulations are performed by varying the operation frequency from 100 Hz to 1000 Hz while keeping the energy deposition (0.0302J), duration of stimulation (1μs) and initial temperature (550K) of flow field constant. The heat transfer coefficient of wall of cavity is 200W/m2K and 500W/m2K separately for comparison. As observed from Figure. 7(a), the peak Mach number is all most same in which maximum change is about 6% with operation frequency of 430 Hz. This is attributed to the same supersonic condition near the orifice. Figure. 7(a) suggests that such boundary conditions do not affect the maximum Mach number in the existing heat transfer coefficient in this paper.

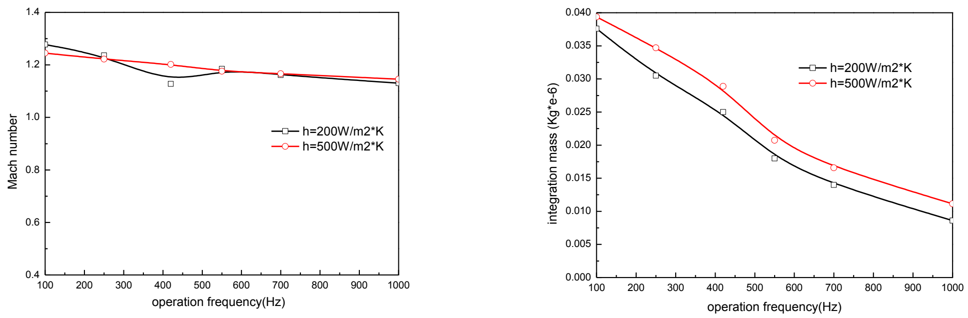

(a) (b)

Fig. 7. Effect of mixed boundary conditions: (a) peak Mach number; (b) the integration mass

As the operation increases, the integration mass of jet variation is from 0.04E-6 Kg (100 Hz) to 0.1 e-6 Kg (1000 Hz) when keep heat transfer coefficient of walls constant of 500W/m2K, as shown in Figure. 7(b). This is attributed to less inhaling duration that is not conducive to sucking of gas outside. Keeping operation frequency constant, increasing heat transfer coefficient can improve the performance, an example is integration mass grow 11% from

200W/m2K to 500W/m2K when operation frequency is 700 Hz. This is because higher heat transfer coefficient of wall of cavity is good to cooling the gas in the cavity during the recovery stage and can inhale more gas from environment.

3.3. Effect of temperature walls

In this series of simulations, the energy deposition (0.0302J) and duration of stimulation (1μs) of flow field was held constant. Operation frequency varies from 100 Hz to 1000 Hz. The initial temperature is equal to temperature of walls which is 550K and 1200K separately for comparison. Figure. 8(a) shows the relationship of temperature of walls and operation frequency. Owing to the same supersonic condition near the orifice, the maximum Mach number is almost same in different existing parameters (maximum change is about 6% with operation frequency of 100 Hz). Care should be taken while designing the shape of orifice so that obtaining larger Mach number of jet, for example Laval nozzle.

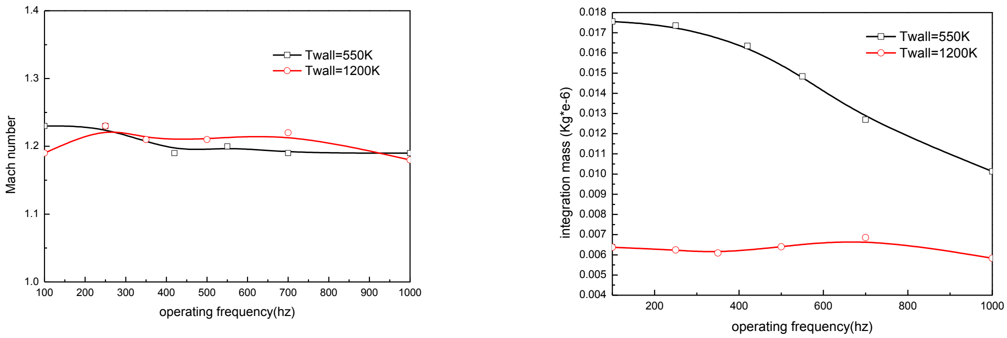

(a) (b)

Fig. 8. Effect of temperature walls: (a) peak Mach number; (b) the integration mass

When Sparkjet actuator operates stably, the exhaling gas mass (the integration mass) is equal to the inhaling gas mass. As the operation frequency increase, the integration mass decreases from 0.0175 e-6 Kg(100 Hz) to 0.011 e-6 Kg with the temperature of 550K(see Figure. 8(b)). This is attributed that decreasing of time interval lower inhaling gas mass from environment with increase of operation frequency. However, if the temperature of walls of cavity is 1200K, the integration mass changes little with operation frequency (about 8%), it means that the performance of actuator is not sensitive to temperature of wall of cavity with this actuator. Figure. 8(b) suggests that lower the temperature of walls can enlarge the strength of Sparkjet because of better cooling condition of air in cavity and walls.

3.4. Dynamic response characteristics of the Sparkjet

Before stimulation of Sparkjet actuator, the whole flow field is quiescent, velocity is 0, pressure, density and temperature is uniform. Investigation of dynamic response particularity is good to understanding of the changing from stimulation beginning to stable operating and operation parameters' impact on performance of actuator and strength of jet. Simulations are performed by varying the operation frequency from 100 Hz to 1000 Hz while keeping the temperature of walls (500K), the energy deposition (0.0302J), duration of stimulation (1μs) and initial temperature (500K) constant in this group. In order to analysis the dynamic response particularity of actuator, this study monitored the relationship of integration mass and momentum and maximum Mach number of the orifice.

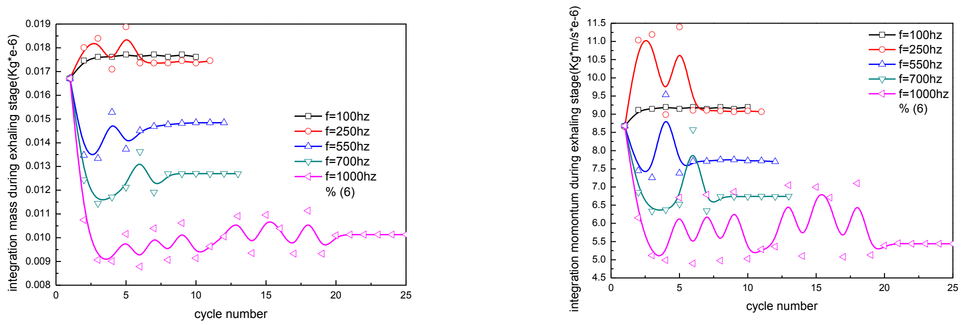

(a) integration mass versus cycle

(b) integration momentum versus cycle

Fig. 9. Dynamic response characteristics of the Sparkjet

Figure. 11(a) shows the integration mass versus cycle number plot with temperature of 550K in the orifice, the integration mass is same at cycle number1 because of same Initial flow field. As the cycle number increase, the integration mass of jet firstly change fluctuant and then prone to a steady value, ultimately they are does not vary with the cycle time which is called dynamic equilibrium. When the two indictors are in dynamic equilibrium, the exhaling gas mass (the integration mass) is equal to the inhaling gas mass, the Sparkjet actuator operates stably. Owning to large operation interval time with small operation frequency, the actuator has enough time in recovery stage to supplement the loss of gas in energy deposition and discharge stage. So it varies from disproportion to stable operation soon, the example is 3 cycle number with 100 Hz. if operation frequency is large, reducing of the inhaling mass during recovery stage lower the gas which remains in the cavity and the integration mass decrease, it result in the more cycle number to operate stably, the example is 20 cycle number with operation frequency of 1000hz.

the integration mass is the function of integration momentum, therefore the relation of integration momentum and cycle number is similar to integration mass ,as shown in Figure. 11(b) . The expression of integration momentum include square of speed and its value is larger than integration mass. if operation frequency is small, integration momentum of stable operation is slightly larger than or equal to cycle number 1. However, integration momentum of stable operation is less than cycle number 1 and performance of the actuator decreases. This is attributed to the time interval of high operation frequency is larger than the first cycle time [15] and the actuator cannot restate the “initial condition”.

in order to gain a clear idea of effect of operation frequency, the time allocation of three energy deposition, discharge and recovery stage in a work period with different operation frequency are also investigated, as observed in Figure. 11. With small operation frequency, The actuator has enough time in recovery stage to “reset”, it means remaining gas mass in the cavity when operating stably and a stimulation completed is equal to remaining gas mass of the first stimulation(Figure. 11(a) and (b)). If time interval is less than the first cycle time (maybe it can be considered be critical frequency, the reciprocal of the first cycle time (Figure. 11(c))), the actuator can be restate the “initial condition”. If the operation frequency is less than the first cycle time, The actuator does not has enough time in recovery stage to supplement the loss of gas in energy deposition and discharge stage. Therefore the integration mass and momentum all decrease with increase of operation frequency (Figure. 11(d))).

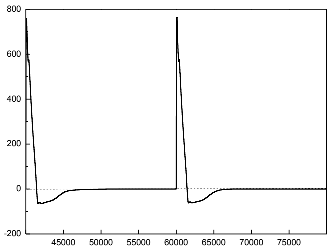

(a) f=100Hz

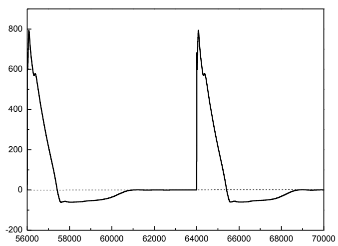

(b) f=250Hz

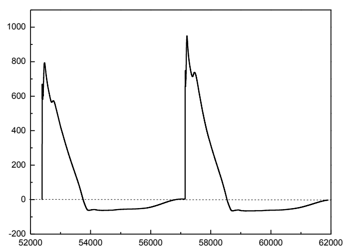

(c) f=420Hz

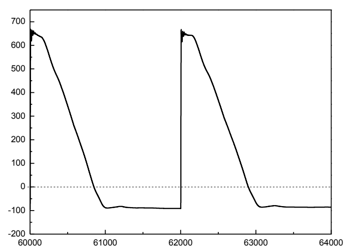

(d) f=1000Hz

Fig. 10. axis velocities versus time with different operation frequency

in addition, the boundary condition of outlet is set temperature of 300K which is less than the initial temperature (500K) in this simulation group. It means that flow field outside the cavity will be cooled from 550K to 300K, and the density near the orifice will increase with same environment pressure (101325Pa). Increasing of density will increase the inhaling gas mass during recovery stage. Figure. 9 shows change of density in flow field. At the time of the 4th work period, density near the orifice is 0.75 Kg/m3 while 1.15 Kg/m3 near the outlet (change about 50%)(Figure. 9(a)). When work period is 25, the density and temperature distribution expect the reign of sparkjet outside cavity has been uniform, as shown Figure. 9(b).

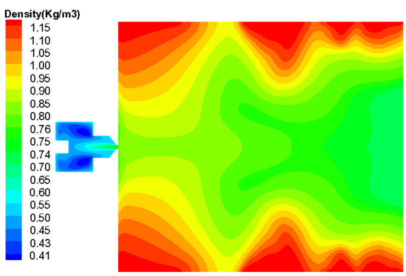

(a) n=4T

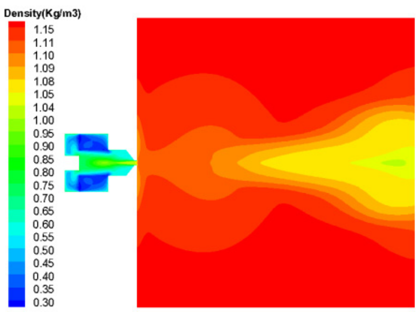

(b) n=25T

Fig .11. density contours at different cycle number（Twall=550K,f=1000Hz）

3.5. Effect of deposition energy

In order to understand the effect of deposition energy, different deposition energy is obtained by changing the magnitude of source term. Deposition energy varies from 0.0015J to 0.08J while temperature of walls (1200K), initial temperature (1200K) and duration of stimulation (1μs) of flow field were held constant. Operation frequency selects 250 Hz and 1000 Hz.

After the baseline actuator operates stably, as the deposition increases, the peak Mach number also increase when the energy is less than 0.02J. However, if energy varies from 0.02J to 0.08J, the maximum Mach number is almost same and up to 1.2, as is shown in Figure. 12. This is due to increase of energy enlarge the pressure gradient in the orifice and yield the more strong Sparkjet. Because supersonic condition occurs near the orifice, this energy or more do not affect the maximum Mach number. Care should be taken while designing the shape of orifice so that obtaining larger Mach number of jet, for example Laval nozzle. Additional, the peak Mach number is not sensitive to operation frequency with different deposition energy.

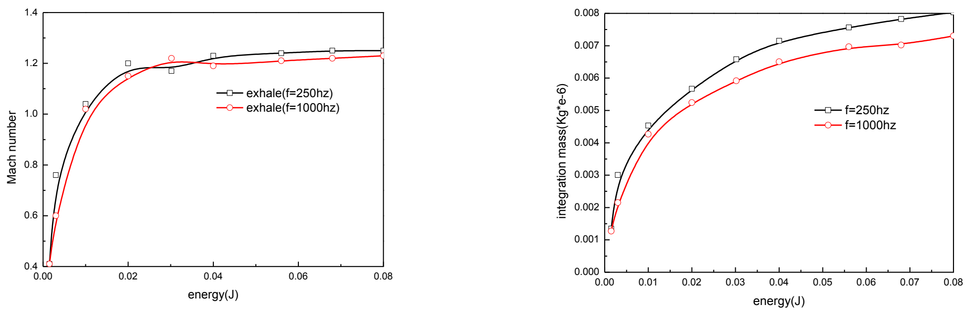

(a) (b)

Fig. 12. Effect of deposition energy: (a) peak Mach number; (b) the integration mass

Figure. 12 shows the integration mass versus deposition energy plot at the orifice. As the as the deposition increases, integration mass also increase while the rate continues to decline. Because deposition energy increases, the pressure in the cavity also increases, therefore the propulsion is stronger. If the energy keeps constant, the integration mass of 250 Hz is larger than1000hz because larger time interval allows longer recovery stage. And the time interval of high operation frequency is larger than the first cycle time and the actuator cannot restate the "initial condition" with 250 Hz.

4. Conclusion and discussion

This study provides a detailed numerical simulation of a swirl-symmetric synthetic jet. The simulation results are compared with the existing experimental and numerical results for the purpose of validation. The user define function (UDF) was applied in the source term of the energy equation to imitate the very arc current discharges. Unlike previous research, this paper come up with two parameters include the integration mass and momentum of air to evaluate the performance of the Sparkjet actuator according to the criterion of the work capacity. This study demonstrates that the boundary conditions of the internal walls of the cavity and energy deposition values have significant impact on the performance of the Sparkjet actuator. The study results in this paper are expressed as follow:

(1) The performance of sparkjet actuator drops rapidly with the increase of operation cycle rapidly and lead the death of its potency when the wall of cavity is adiabatic because of no heat transfer in walls and gas.

(2) Keeping the temperature of walls constant, if temperature is small, the integration mass and momentum during the exhaling stage decrease with the increase of temperature with small temperature of walls. The performance of actuator is not sensitive to temperature of wall of cavity if the temperature of wall of cavity is higher.

(3) If the wall of cavity is set to be coupled with effect of radiation and convection, the performance of actuator decreases with heat transfer coefficient.

(4) From stimulation beginning to stable operating, different operation cycle is undergone in different operation frequency and is related with the first cycle time and the time interval between discharges (stimulation). When the two indictors are in dynamic equilibrium, the exhaling gas mass (the integration mass) is equal to the inhaling gas mass, the Sparkjet actuator operates stably. When the first cycle time is larger than time interval between discharges, the actuator is able to recover to the initial state, the actuator can "reset". The operation cycle increase with increase of operation frequency when the first cycle time is less than time interval between discharges, the actuator cannot "reset".

(5) The performance of actuator increases with increase of deposition energy.

Acknowledgment

The authors gratefully acknowledge the financial support for this project from National Natural Science Foundation of China, NO.51306088; NO.51106073; Natural Science Foundation of Jiangsu Province, No. BK20130790.

5. Reference

[1]Smith B L, Glezer A. vectoring and small-scale motions effected in free shear flows using synthetic jet actuators[J]. AIAA Paper ,1997,0657:213-241.

[2]Amitay, M., Smith, B. L., and Glezer, a. aerodynamic flow control using synthetic jet technology[J]. AIAA Paper, 1998, 0434 .

[3]Smith B L, Glezer A. The Formation and Evolution of Synthetic Jets[J].Physics of Fluids, 1998, 10(9): 2281-2297.

[4]Chen, Y. , Liang, S. , Aung, K. , Glezer, A. , Jagoda, J. enhanced mixing in a simulated combustor using synthetic jet actuators[J].AIAA Paper , 1999,0489.

[5]Honohan, A. M., Amitay, M., and Glezer, A. aerodynamic control using synthetic jets[J]. AIAA Paper , 2000, 0554.

[6]Chatlynne, E. , Rumigny, N. , Amitay, M. , Glezer, A . virtual aero-shaping of a clark-y airfoil using synthetic jet actuators[J] , AIAA Paper, 2001,0732:425-444.

[7]Anna Pavlova, Michael Amitay. electronic cooling using synthetic jet impingement[J]. AIAA Paper, 2006,1546 .

[8]S.R. Fugal, B.L. Smith, R.E. Spall, Displacement amplitude scaling of a two dimensional synthetic jet, Phys, Fluids 17 (2005) 045103.

[9]H. Tang, S. Zhong, 2D numerical study of circular synthetic jets in quiescent flows, Aeronaut. J. 109 (2005) 89.

[10]D. Caruana, P. Barricau, P. Hardy. The "Plasma Synthetic Jet" Actuator: Aero-thermodynamic Characterization and first Flow Control Applications, 47th AIAA Aerospace Sciences Meeting Including The New Horizons Forum and Aerospace Exposition, Orlando, Florida, AIAA 2009-1307, January 2009.

[11]K. R. Grossman, B. Z. Cybyk, and D. M. VanWie, Sparkjet actuators for flow control, 41st AIAA Aerospace Sciences Meeting and Exhibit, 2003-57, 2003.

[12]K. R. Grossman, B. Z. Cybyk, M. C. Rigling, and D. M. VanWie, Characterization of sparkjet actuators for flow control, 42nd AIAA Aerospace Sciences Meeting and Exhibit, 2004-89, 2004.

[13]Wang Lin and Luo Zhen-Bing, Energy efficiency and performance characteristics of plasma synthetic jet, Acta Phys. Sin, Vol. 62, No. 12 (2013) papge 125207-1 to 125207-10.

[14]Shan Y, Zhang J Z, Tan X M Numerical study of the flow characteristics and excitation parameters for the spark jet actuator 2011 J. Aero. Power 26 551 (in Chinese).

[15]Yuanwei LV, Jingzhou ZHANG, Yong SHAN, A numerical investigation of the Sparkjet flow in single-shot mode, The Heat Transfer Symposium 2014, Beijing, China, 6-9, May, 2014.

[16]B. Z. Cybyk, J. T. Wilkerson, and K. R. Grossman, Performance characteristics of the sparkjet flow control, 2nd AIAA Flow Control Conference, 2004-2131, 2004.

[17]Sarah J Haack, Trent Taylor, Jerry Emhoff and Bohdan Cybyk, Development of an Analytical Sparkjet Model, 5th Flow Control Conference 28 June - 1 July 2010, Chicago, Illinois, AIAA 2010-4979.

[18]S. J. Haack, T. M. Taylor and B. Z. Cybyk, Experimental Estimation of Sparkjet Efficiency, 42nd AIAA Plasmadynamics and Lasers Conference, 27 - 30 June 2011, Honolulu, Hawaii, AIAA 2011-3997.

[19]ANSYS Fluent v12.0 Software User's Gide, 2009.